

Growth and Electrical Characterization of TlInTe₂ Single Crystal

A. A. Al-Ghamdi, A.T. Nagat⁽¹⁾, F.S. Al-Hazmi S. Al-Heniti, F.S Bahabri⁽²⁾, M.M. Mobarak and S.R. Alharbi

Physics Department, Faculty of Science, King Abdulaziz University

*1- Physics Department, Girls Colleges of Education in Jeddah,
Saudi Arabia*

*2-Physics Department, Faculty of Science, South Valley University,
Qena, Egypt*

Abstract. High efficiency design for single crystal growth from melt based on Bridgman technique is constructed locally and used for growing TlInTe₂ crystals. Measurements of Hall coefficient and DC electrical conductivity covering a temperature range from 158 to 473 K were conducted. The investigated samples have P-Type conductivity with R_H of 2.3×10^9 cm³/coul. at room temperature and carrier concentrations as 2.81×10^9 cm⁻³. Energy gap ΔE_g and ionization energy ΔE_a were estimated as 0.72 eV and 0.113 eV, respectively. The diffusion coefficient, diffusion length, as well as relaxation time were evaluated, and the scattering mechanism of charge carrier was checked.

1. Introduction

The chalcogen compounds formed from elements of group III and VI of the periodic table are of particular interest because of their practical applications in different fields, such as electronic devices, refrigerating materials, photovoltaic detectors, and optical devices^[1].

* Correspondent author. E mail:” Aghamdi90@hotmail.com”

Most of the technological electronic and opto-electronic applications utilize semiconductor materials in crystalline forms. The discovery of new semiconductor materials on the basis of $A^{III} B^{III} C_2^{VI}$ is an urgent problem due to the reliability of these compounds in solid – static electronics. $TlInTe_2$ belongs to the family $^{[2-1]} Tl AX_2$ (A : In, Ga; X : S, Se, Te).

It forms a tetragonal lattice of group symmetry $D_{4h}^{18}-14/ mcm$, therefore it is structurally analogous to $TlSe$. In $TlInTe_2$ four Te atoms form a tetrahedron with a strongly bound In^{+3} – ion in its centre. This tetrahedron forms covalent $[In^{3+}Te_2^{2-}]^1$ chains parallel to the C–axis of the crystal. They are bonded to each other by Octahedrally arranged Tl^{1+} – ions by means of weak ionic bonds. The resulting lattice exhibits a one – dimensional organization, which is responsible for the fibrous structure of the material.

$TlInTe_2$ is a P-Type semiconductor with a fibrous structure which sometimes is referred to as being quasi – one – dimensional. Numerous studies determined physical and crystallographic data such as melting point, density or form and size of the crystal cell, infrared reflection spectra and nonlinear electrical behavior^[3-8]. Other investigations analyzed properties of the electronic band structure like energy gaps, positions of acceptor levels and carrier concentration^[9-12].

$A^{III} B^{III} C_2^{VI}$ compounds are formed in layered – chain structure as $A^{III} C^{VI} – B^{III} C^{VI}$ in which the components $^{[13]} A^{III} C^{VI}$ and $B^{III} C^{VI}$ have the ratio 1:1. For instance, in compounds $TlInTe_2$ the components are arranged in the form $TlTe–InTe$ and are called the ternary - chain $TlInTe_2$ – Type.

The transport properties of $TlInTe_2$ single crystals are not well known and a scan of literature reveals no reports available on Hall coefficient and electrical conductivity. The intention of this report is to describe a low cost, high efficiency and local design for single crystal growth from melt and study the electrical conductivity and Hall effect in order to draw an accurate picture about the actual behavior of this compound.

2. Experimental Procedure

2.1 Design of Crystal Growth

The essence of technological advance lies in the ability of manufacturing to produce single crystal material, melt growth is undoubtedly the best method available today for congruently melting materials. The design of good equipment needs consideration for creating and controlling the environment in which a crystal with desired properties can grow. A special design for crystal growth from melt using Bridgman technique is constructed locally for the performance of the present work. It demonstrates that the driving force required for moving the loaded ampoule is equivalent to the decrease of water level drained in a special container which in turn indicates the rate of motion. This design consists of the following parts:

2.2.1 Mechanical System

This system consists of two wheels, one is fixed at the center of the higher end of the furnace, whereas the other is fixed at the center of the furnace lower end. These wheels can easily be moved, and each contains a groove through which a wire passes to draw the sealed vacuumed ampoule charged with the desired material for growing. The ampoule is tied at its two ends hooks with a suitable wire extended toward the two ends of the furnace. Equilibrium position for the ampoule at the center of the furnace can be reached by the use of suitable weights, attached at the far ends of the wire.

The lower end of the wire is connected to a suitable weight held on a bridge made from a material that can easily rest and float on a surface of water in filled water glass container. The water is allowed to discharge down in the form of drops at slow rate through a water valve, and thus the weight drops down pulling down the wire together with the ampoule in the furnace from zone to zone. The container valve controls the water drops in such a way that an amount of water decreases gradually and slowly with the required rate, and consequently the charged ampoule moves down gradually in slow motion from zone to zone inside the furnace.

2.2.2 The Electrical System

This system consists of a silica tube furnace with three zones. The furnace of 80cm length and 5cm diameter is covered with a mica sheet

and asbestos, followed by a Nichrome wire with diameter 1.5mm wound on the tube in such a manner that the distance between the wound wires varied from zone to another. In every zone a symmetry wound wire is used to produce homogenous temperature in the required zone. The upper zone is designed as to produce temperature higher than the melting point of the required composition and the middle zone is designed to produce temperature corresponding to the melting point. The lower zone is designed to produce temperature lower than melting point of the desired growing material. The temperature of the three zones may be controlled by variance transformer. The temperature may be measured by means of chromel – Alumel thermocouple.

2.3 Crystal Growth of $TlInTe_2$

A compound of $TlInTe_2$ in stoichiometric ratio is prepared by direct melting in a quartz ampoule. The ampoule was constructed with a sharp end at the bottom to facilitate seeding in the growth process. Before charging ampoule with the material it is washed with pure alcohol and hot distilled water, then coated with a thin layer of graphite to prevent contamination of material on the internal surface of the ampoule. The ampoule is charged with the material, evacuated to about 10^{-5} torr then sealed. The required amount of materials (Aldrich Mark, purity 99.999%) is 17.7925g of pure thallium representing 35.585%, 9.993g of pure indium representing 19.986% and 22.214g of pure tellurium representing 44.429%.

At the beginning of growth the ampoule was held in the hot zone of the furnace at 1137 K (24h) for melt homogenization. The melt is then shaken gently during heating several times to accelerate the diffusion of the constituents through each other. With the aid of the mechanical system the ampoule with its charge is driven to the next zone. The temperature in this region is corresponding to the melting point (1045 k) according to the phase diagram ^[15]. The growth rate during the experiment is 2.2 mm/h. Since the third zone temperature was less than the melting point, the crystallization proceeds till the contents solidify. The product crystal was obtained with 1.5cm diameter and nearly 10cm length. Details of their process were described elsewhere ^[16]. The

resulting ingot was identified with X-ray diffraction analysis. X-ray chart is illustrated in Fig.1. Samples are single crystals, grey, good quality and had a metallic glitter. The results were in good agreement with the published values [6].

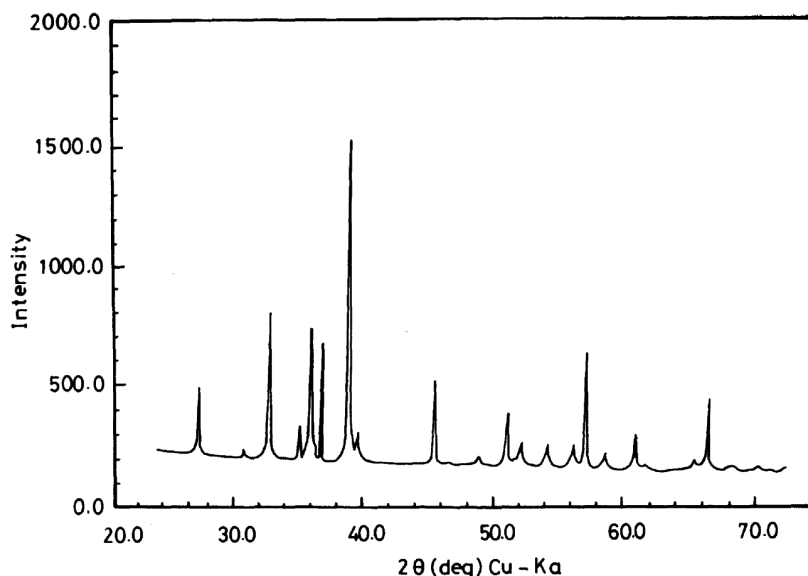


Fig. 1. X-ray diffraction for TlInTe_2 single crystal.

2.4 Electrical Conductivity and Hall Effect of TlInTe_2

A Pyrex glass cryostat was designed for the purpose of measuring the electrical conductivity and Hall coefficient in a wide range of temperature under vacuum [17]. The samples were in the form of rectangular parallelepiped of dimensions $0.45\text{cm} \times 0.1\text{cm} \times 0.15\text{cm}$. Silver paste was used as a good Ohmic contact on both sides of TlInTe_2 samples, checked by the current–voltage characteristics measurements. Measurements were carried out under vacuum to avoid sample oxidation (in high temperature range) and to prevent water vapor condensation (in low temperature range).

Measurements above room temperature were carried out with the help of electrical insulator heater. Liquid nitrogen was introduced in the cryostat reservoir for low temperature measurements. A field of about 5 kilogauss was obtained from CGNCO electromagnet with its suitable regulated and stabilized power supply.

Hall voltage was taken as an average of four readings, using a reverse switch to reverse direction of current as well as that of magnetic field and to avoid Nernst and magnetoresistance effects. This is the method of making DC ^[18] Hall measurements recombined in ASTM F 76. The specimen temperature was measured with the aid of copper constantan thermocouple. Measurements were done in a wide temperature range extending from 158 to 473 K.

3. Results and Discussion

The effect of ambient temperature on the electrical conductivity of TlInTe₂ single crystal has been investigated. Figure 2 shows a plot of the electrical conductivity versus the inverse absolute temperature. The curve shows a typical semiconductor behavior. At low temperature (the extrinsic region) the carrier concentration may be determined by the number of ionized acceptors, since the main part will be played by free carrier transition from the impurity level, and consequently the conductivity increases slowly.

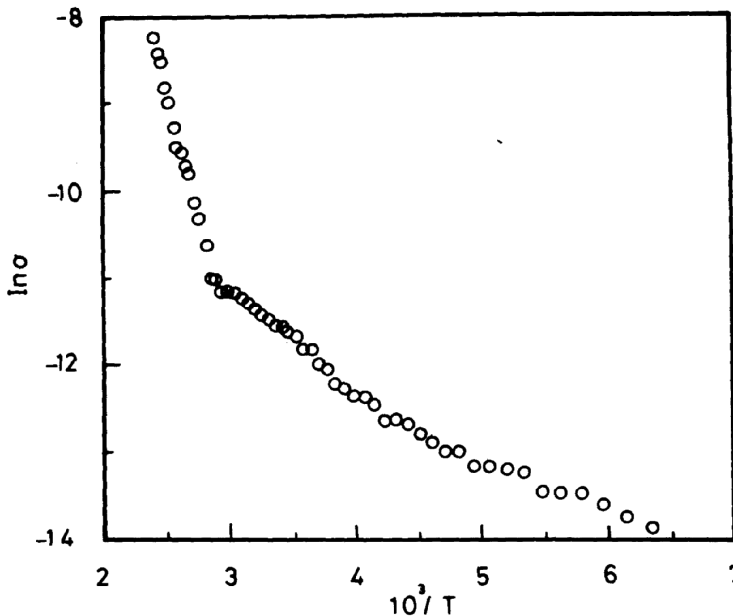


Fig. 2. A plot of the electrical conductivity versus the inverse of absolute temperature for TlInTe₂.

The impurity ionization energy ΔE_a is calculated, and was found to be 0.1158 eV. At high temperature region (357-473 K) the conductivity rises very rapidly due to the rapid increase in total carrier density. This indicates that the intrinsic conductivity becomes more favorable at high temperatures. The energy gap width was deduced as 0.73 eV. The presence of the intermediate region is also seen between 250 and 357 K.

The transition temperature from impurity to intrinsic conductivity depends on the concentration of impurity in the specific semiconductor, and on the forbidden bandwidth for a fixed impurity concentration. In this middle zone the rise in the electrical conductivity is due to an increase in mobility, since the carrier density in this temperature region remains practically constant until the intrinsic region is reached. The temperature dependences exhibit a transition from a region of lower slope to one of higher slope.

At room temperature the conductivity of TlInTe₂ specimen is $9.59 \times 10^{-6} \Omega^{-1} \text{ cm}^{-1}$. Figure 3 represents the relation between Hall coefficient and temperature for the investigated sample.

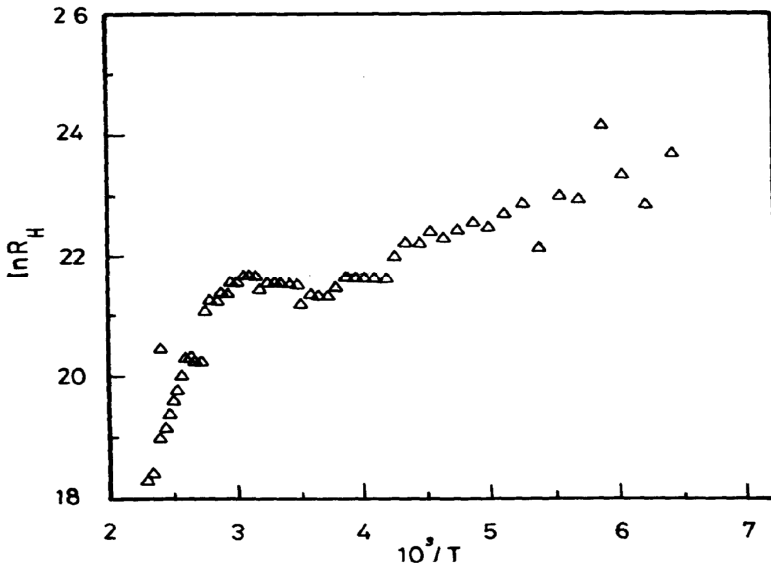


Fig. 3. Relation between Hall effect and temperature for TlInTe₂

The Hall coefficient at room temperature R_H is evaluated as $2.3 \times 10^9 \text{ cm}^3/\text{C}$. The investigated sample turned out to be a P-type. From the curve in Fig. 3 the three regions can clearly be distinguished. The

intrinsic region is the region in which the Hall coefficient varies linearly and rapidly with temperature, while in the impurity region it varies slowly with temperature. An intermediate region is observed between these two regions.

Figure 4 represents the relation between $R_H T^{3/2}$ and $10^3/T$. It can be divided into two parts, the first part at low temperature where $R_H T^{3/2}$ decreases slowly with increasing temperature. This region indicates the extrinsic part from which the position of the acceptor level is calculated as $\Delta E_a = 0.11\text{eV}$. The second part is above 360 k, a region in which the $R_H T^{3/2}$ decreases rapidly as the temperature increases, referred as the intrinsic region. The forbidden-band width is calculated from these graphs giving a value of 0.71eV. The forbidden zone width as deduced from Hall measurements is in a reasonable agreement with that deduced from the conductivity data and in good agreement with the published^[11] values. The mobility of charge carriers may be determined from simultaneous measurements of conductivity and Hall constant.

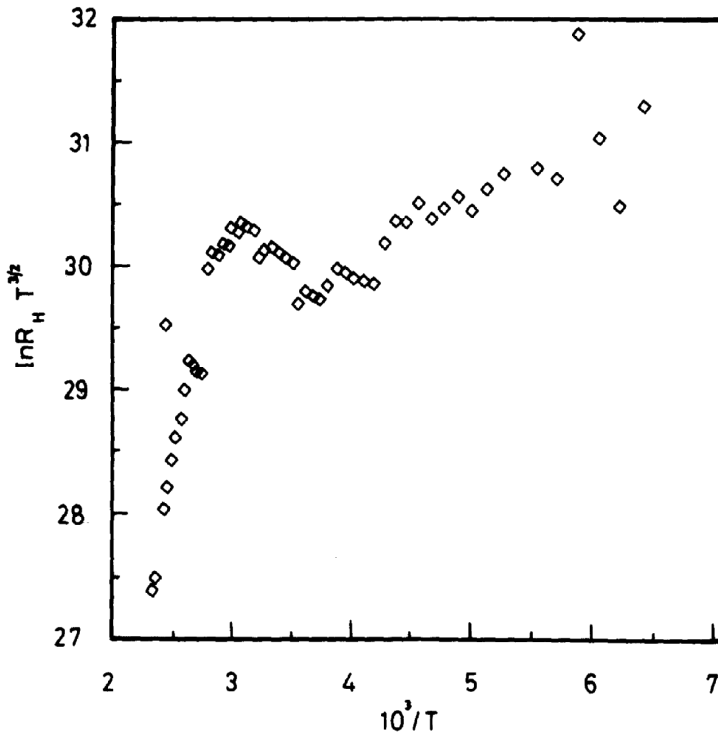


Fig. 4. Relation between $R_H T^{3/2}$ and $10^3/T$.

Figure 5 shows the temperature dependence of the Hall mobility of current carriers in TlInTe₂ crystals. As is shown the mobility increases with temperature according to $\mu \propto T^{3/2}$. Such behavior is characteristic of scattering mechanism of charge carriers with ionized impurity, since the exponent value and its sign suggest such mechanism of scattering. At room temperature the mobility of charge carriers can be determined as 21291.23 cm²/V.sec. The charge carrier mobility in TlInTe₂ is much higher than other semiconducting materials [19] formed from A^{III} B^{VI} group.

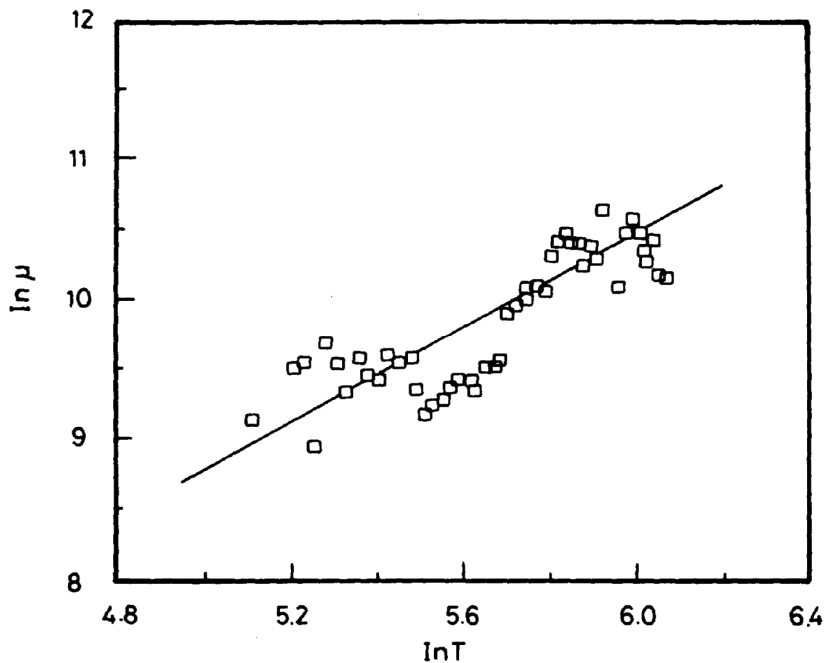


Fig. 5. Temperature dependence of Hall mobility of current carriers for TlInTe₂.

Hall measurements are very useful technique in studying the temperature effect on the carrier concentrations. This is illustrated in Fig. 6, where the concentration of hole carriers in the high temperature region increases rapidly with temperature but increases slowly with temperature in the low temperature region.

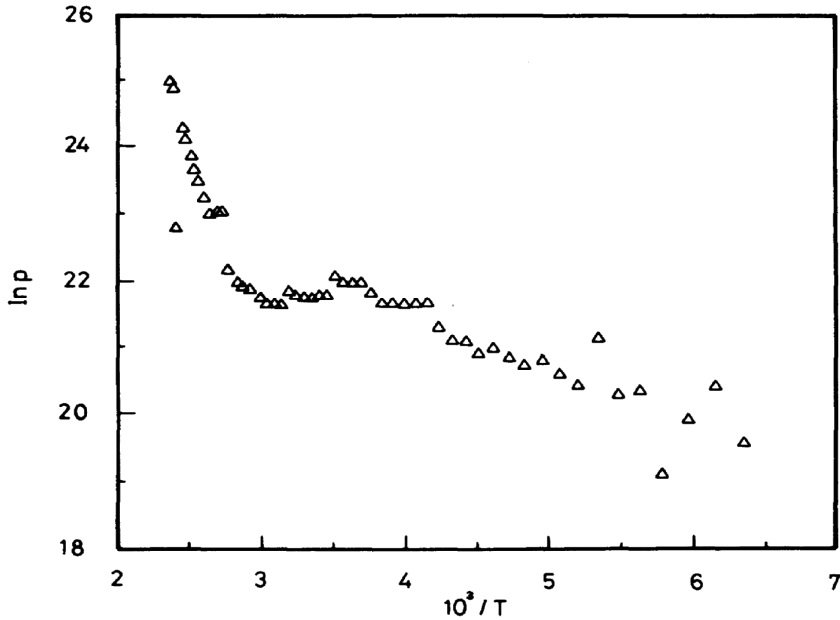


Fig. 6. Hole concentration versus reciprocal temperature for TIInTe₂.

The carrier concentrations at 300 K as calculated from Hall coefficient is $2.81 \times 10^9 \text{ cm}^{-3}$. The calculated diffusion coefficient for holes is $551.4 \text{ cm}^2/\text{sec}$. The relaxation time as well as diffusion length of holes deduced at room temperature is calculated as $1.2 \times 10^{-11} \text{ sec}$ and $8.176 \times 10^{-5} \text{ cm}$ respectively.

Acknowledgment

The authors would like to thank Prof. S.A. Hussein for fruitful discussions. Two of the authors (Prof. A. Al-Ghamdi & Prof. Nagat) would like to thank the deanship of research at King Abdulaziz University for supporting part of this work on the form of project on 2006.

References

- [1] Romermann, F., Feutelais, Y., Fries, S.G and Blachnik, R., *Intermetallics*, **8**: 53 (2000).
- [2] Watzke, O., Schneider, T., and Martienssen Chaos, W., *Solitons and Fractals*, **11**: 1163 (2000).
- [3] Vinogradov, E.A., Grasanly, N.M., Dzhavadov B.M. and Tagirov, V.I., *Sov. Phys. Solid State*, **21**: 1607 (1979).

- [4] Gasaney, N.M., Dzhavadov, B.M., Tagirov, V.I. and Mavrin, B.N., *Fizika*, **3**: 106 (1979).
- [5] Sastry, V.B. Murthy, K.S. Mamedov, N.T. and Prabhavathy, *Phys. Stat. Sol. (a)*, **110**: 5 (1988).
- [6] Banys, J., Wondre, F.R. and Guseinov, G., *Materials Letters* **7**: 269 (1990).
- [7] Harias, M.P., Kalomiros, J.A., Ch. Karakotsou, Anagnostopoulos, A.N. and Spyridelis, J., *Phys. Rev. B* **49**: 1699 (1994).
- [8] Gospodinov, M. M., Stoyanova, V.B. and Yanchev, I. Y., *Materials. Res. Bull.*, **1**: 1635 (1997).
- [9] Hantias, M.P., Anagnostopoulos, A.N. and Kambas, K.J., *Spyrielleis Physica B*, **160**: 154 (1989).
- [10] Hantias, M.P., Anagnostopoulos, A.N. and Kambas, K., Spyrididis, J., *Phys. Rev. B* **43**: 4135 (1991).
- [11] Abay, B., Gurbulak, B., Yidirim, M., Efeoglu, H., Tuzemen, S. and Yogustcu, Y.K., *J. Electronic Materials*, **25**: 1054 (1996).
- [12] Wakita, K., Shim, Y., Grudzhev, G., Mamedov, N. and Hashimzade, F., *Phys. Stat. Sol. (a)*, **203**: 2841 (2006).
- [13] B. Gurbulak, *Physica B*, **293**: 289 (2001).
- [14] Subbarao, E.C. Singhal, L.K. Chakmovorty, D., Merrian F. and Raghavan, V., *Experimental in Materials Science*, MC Graw– Hill INC, (1972).
- [15] Gurbulak, B., Coskan, C., Kogan, S., Ates, A. and Yogurtecu, Y.K., *Tur. J. Phys.*, **24**: 29 (2000).
- [16] Hussein, S.A. and Nagat. A.T., *Cryst. Res. Technol.*, **24**: 283 (1989).
- [17] Hussein, S. A., *Cryst. Res. Technol.*, **24**: 6 (1989).
- [18] Runyan, W.R., *Semiconductor Measurements and Instrumentation*, Tokyo (1976).
- [19] Nagat, A. T., *J. Phys. Condens. Matter*, **1**: 7921 (1989).

إنماء ودراسة الخواص الكهربائية لبلورة $TlInTe_2$ أحادية الطور

أحمد الغامدي ، وفرج الحازمي، وصالح الحنيطي، ونجاة توفيق^(١) وفاطمة باهبري^(٢)، مصطفى مبارك^(٣) و سهام الحربي^(٤)

قسم الفيزياء، كلية العلوم- جامعة الملك عبدالعزيز،

و^(١) قسم الفيزياء، كلية التربية للبنات - جدة - المملكة العربية السعودية،

و^(٢) قسم الفيزياء، كلية العلوم، جامعة جنوب الوادي، قنا، جمهورية مصر

العربية

المستخلص. تم بناء وتصميم جهاز عالي الكفاءة لإنماء بلورات $TlInTe_2$ أحادية الطور على طريقة بريد جمان محلياً. تمت دراسة الموصلية الكهربائية ومعامل هول لهذه البلورات، في المدى من درجات الحرارة ١٥٨-٤٧٣ كلفن. من خلال دراسة الموصلية تبين أنها من نوع P-type، وأن قيمة معامل هول $R_H=2.3 \times 10^9$ cm^3/C عند درجة حرارة الغرفة، وتركيز ناقلة الشحنة هو 2.81×10^9 cm^{-3} . كما تم تعيين اتساع طاقة الفجوة ΔE_g ، وكذلك طاقة التأيين لتكونا 0.72eV و 0.113eV على التوالي. كما أن معامل الانتشار، و طول الانتشار، وزمن الاسترخاء تم تعيينهم في هذه الدراسة مع التأكد من ميكانيكية تشتت الشحنات.